Rev. Adv. Mater. Sci. 28 (2011) 64-68

INFLUENCE OF LEAD ON SURFACE OXIDE OF Ni-BASED ALLOY IN A CAUSTIC SOLUTION

Dong-Jin Kim, Hyun Wook Kim, Sung-Woo Kim and Hong Pyo Kim

Nuclear Materials Research Division, Korea Atomic Energy Research Institute (KAERI), 1045 Daedeok-daero, Yuseong-gu, Daejeon, 305-353, Korea

Received: February 17, 2011

Abstract. Degradation of Ni based alloys as steam generator tubing material starts from a modification of thin surface oxide by lead. This work focuses on analyzing the surface oxide for Ni based alloys in 0.1M NaOH solution at 315 °C using potentiodynamic curve, TEM and TEM-EDS. It was found that the Cr rich oxide played an important role in SCC resistance. Pb was effectively examined in the oxide at the tight crack tip as well as free surface oxide.

1. INTRODUCTION

Nickel based Alloy 600 (Ni 75 wt.%, Cr 15 wt.%, Fe 10 w.t%) and Alloy 690 (Ni 60 wt.%, Cr 30 wt.%, Fe 10 wt.%) as an alternative of Alloy 600 have been used for the heat exchanger tubes of the steam generators (SGs) in nuclear power plants, which are operated at a high temperature and a high pressure above 300 °C and 100 bar.

In spite of much effort to reduce the material degradations, stress corrosion cracking (SCC) is still one of important problems to be overcome. Especially, lead is known to be one of the most deleterious species in the reactor coolants that cause SCC of the alloy [1-4]. Even Alloy 690 having superior SCC resistance is also susceptible to lead in alkaline solution [5,6].

Cracks can initiate and propagate through unavoidable breakdowns and alterations of a surface oxide formed naturally on Alloy 600 in an aqueous solution. Therefore the correlation of oxide property with SCC behavior is pre-requisite to mechanistic understanding of PbSCC.

This work analyzes the surface oxide for Ni based alloys in 0.1 M NaOH solution at 315 °C using potentiodynamic curve, TEM, and TEM-EDS (energy dispersive X-ray spectroscopy).

2. EXPERIMENTAL

The test specimens were fabricated from 19.05 mm outside diameter Alloy 600 steam generator tubing materials which were thermally treated (TT) at 704 °C for 15 h after solution annealing at 975 °C for 20 min for immersion and potentiodynamic tests and high temperature mill annealed (HTMA) at 1024 °C for 3 min for SSRT test, respectively. The TT Alloy 690 was thermally treated at 715 °C for 10 h after solution annealing at 1105 °C for 2 min.

The 0.1M NaOH solution was made using high-purity water [room temperature resistivity of 18 MΩ·cm]. Reagent grade PbO was added to the caustic solution at an amount of 10,000 ppm as a source of lead. Deaeration was accomplished by a high purity nitrogen gas purging for 24 h.

The slow strain rate tension (SSRT) test was performed for uniaxial tension specimens fabricated from the nickel based alloys in the unleaded and leaded solutions. The tests were carried out in 1 L nickel autoclaves at 315 °C and an equilibrium pres-

Corresponding author: Dong-Jin Kim, e-mail: djink@kaeri.re.kr

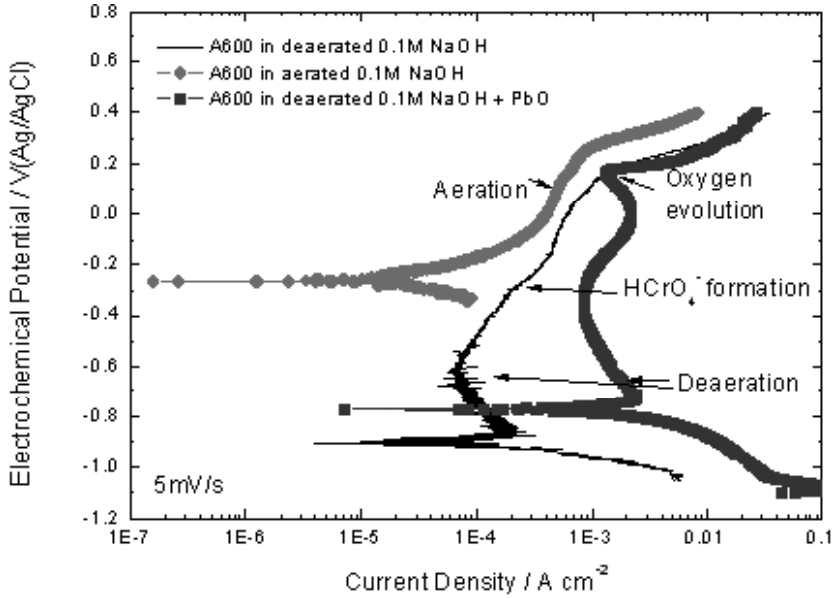

Fig. 1. Potentiodynamic curves for Alloy 600 in 0.1 M NaOH at 315 °C as a function of PbO addition and dissolved oxygen.

sure. The test specimens were immersed at an open circuit potential (OCP) without an impressed electrochemical current. The strain rate was $2x10^{-7}$ s^{-1}.

The immersion test and potentiodynamic test were carried out for rectangular plate specimens (10 mm x 10 mm) fabricated from the tubing. The surface of the specimens was polished up to 1 μm using a diamond suspension. An Alloy 600 wire was spot welded to the specimen, and the wire was shielded with a heat-shrinkable PTFE tubing. The immersion test was performed in a 1-gallon nickel autoclave at 315 °C for 14 days. The potentiodynamic test was carried out using Ag/AgCl external electrode as a reference electrode and Pt wire as a counter electrode in a 1-gallon nickel autoclave at 315 °C with the scan rate of 5 mV/s using a Solartron 1287 electrochemical interface.

After the immersion test, the surface oxide layer and its composition was examined by using a field emission transmission electron microscopy (TEM), equipped with an energy dispersive X-ray spectroscopy (EDS) (JEM-2100F). The crack tip was also observed using the SSRT tested specimen.

3. RESULTS AND DISCUSSION

The SSRT test results obtained in various aqueous solutions are summarized in Table 1 for Alloy 600 and Alloy 690. High temperature pH was obtained using MULTEQ [7]. SCC ratio is defined as SCC area over cross section area of the specimen obtained from the observation of fracture surface. Elongation to rupture was determined from the stress-strain curve. Elongation to rupture as well as SCC ratio can be used as criteria for SCC susceptibility based on the fact that yield strength and tensile strength are decreased with the stress corrosion cracking leading to the lower elongation to rupture.

The SCC susceptibility for Alloy 600 was greatly increased to 78% by adding PbO to the 0.1M NaOH where Alloy 600 does not show SCC while there is little SCC for Alloy 690 in 0.1 M NaOH, irrespective of PbO addition. Moreover PbSCC occurs more severely in deaerated solution (78%) than non-deaerated solution (48%).

Fig. 1 shows potentiodynamic curves for Alloy 600 in 0.1 M NaOH at 315 °C as a function of PbO addition and dissolved oxygen. OCP was observed at -0.9 V(Ag/AgCl) in unleaded 0.1 M NaOH solution. Passive-active transition, passive region and transpassive region due to oxygen evolution were shown with the increase of applied potential. By adding PbO to 0.1 M NaOH, passive current was significantly increased indicating that the oxide passivity greatly degrades by the addition of PbO. The OCP was increased from -0.9 to -0.8 V(Ag/AgCl). The equilibrium electrochemical potential of Pb^{2+}/Pb is higher than the equilibrium potential of Ni^{2+}/Ni [8]. As a result, the OCP of Alloy 600 is higher in the leaded solution. It is notable that the aqueous form of Cr such as $HCrO_4^-$ can be dissolved around -0.2 V(Ag/AgCl).

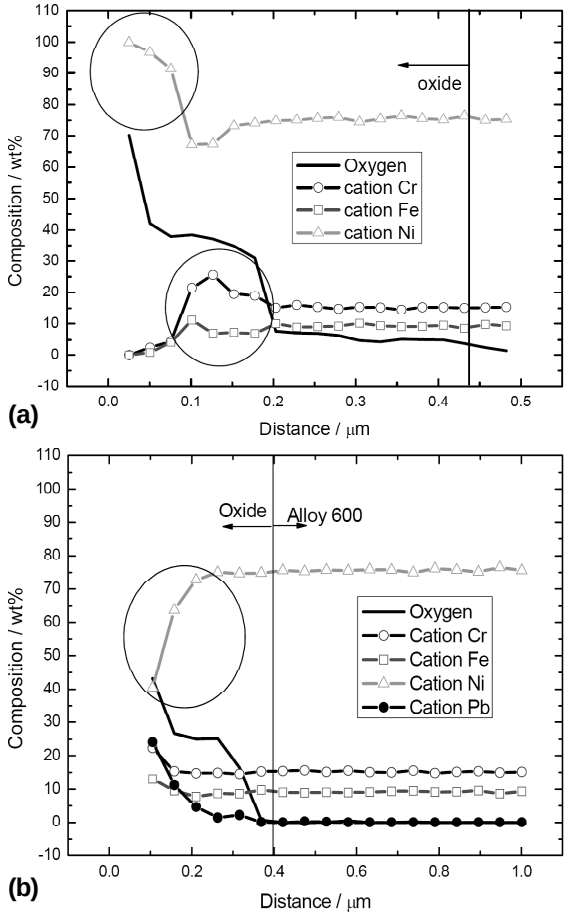

Fig. 2. The chemical compositions for the surface oxide layer formed on the Alloy 600 specimens at 315 °C; (a) 0.1 M NaOH and (b) 0.1 M NaOH + PbO.

From the results of Table 1 and Fig. 1, it is conceived that the degradation of the passivity caused by the Pb addition to the solution is closely related with the increased SCC susceptibility. Lead ions can reportedly be incorporated into the oxide producing dissolution of metal composed of Alloy 600. This can introduce a lattice mismatch which in turn degrades the passivity of the oxide. As the lead is incorporated into the oxide as an oxide state, lead can also degrade the passivity. This degradation of the passivity caused the degraded SCC resistance for Alloy 600 in the leaded solution [9].

In 0.1 M NaOH without deaeration, OCP was around -0.3 V(Ag/AgCl) which is much higher than active-passive region. From this, the electrodeposition of Pb is not available and the oxide film can be formed at an OCP in non-deaerated 0.1 M NaOH solution with PbO leading to less PbSCC susceptibility than that in deaerated solution as shown in Table 1. However it was reported [9] that lead also affects the oxide degradation even in leaded solution without Pb electrodeposition according to the experimental results of current transient experiment. This can cause PbSCC in the non-deaerated leaded solution.

Fig. 2 shows the TEM-EDS results for the Alloy 600 specimens immersed in the unleaded 0.1 M NaOH solution (Fig. 2a) and in the leaded solution (Fig. 2b). Duplex oxide layer of the outer Ni-rich oxide and the inner Cr-rich oxide (~30 wt.%) is observed in the unleaded 0.1 M NaOH solution while a single layer was observed in the leaded 0.1 M NaOH solution. In the leaded solution, a large amount of lead was observed at about 25% on the surface. As a result, Ni was depleted in the oxide layer and the Cr-rich oxide was not observed. The Cr concentration in the oxide formed in the leaded 0.1 M NaOH solution was almost the same as the concentration of Alloy 600 matrix except for near oxide surface region. From the results of Figs. 1 and 2, the du-

Table 1. Elongation to rupture and SCC ratio obtained from the SSRT test in various aqueous solutions at 315 °C.

Environment	Elongation to rupture (%)	SCC ratio	pH (315 °C) by MULTEQ	Remark
-0.1 M NaOH (Deaeration)	57	~0	9.9	Alloy 600
-10,000 ppm PbO addition (Deaeration)	24	78	9.9	
-10,000 ppm PbO addition (Non-deaeration)	35	48	9.9	
-0.1 M NaOH (Deaeration)	59	~0	9.9	Alloy 690
-0.1 M NaOH + 10,000 ppm PbO addition (Deaeration)	55	1.4	9.9	
-0.1 M NaOH + 10,000 ppm PbO addition (Non-deaeration)	54	1.4	9.9	

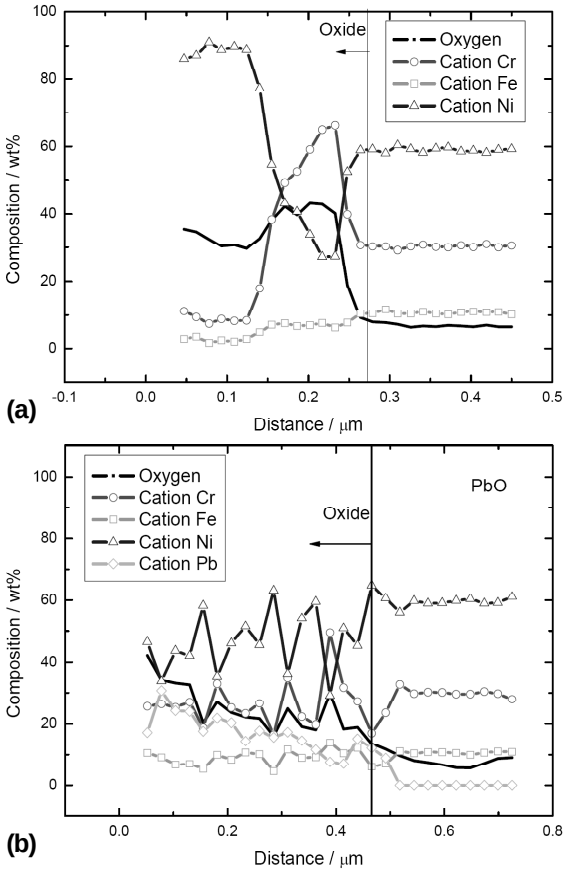

Fig. 3. The chemical compositions for the surface oxide layer formed on the Alloy 690 specimens at 315 °C; (a) 0.1 M NaOH and (b) 0.1 M NaOH + PbO.

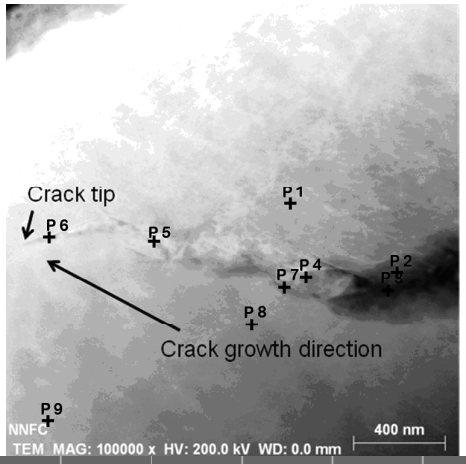

Positions	O	Cr	Fe	Ni	Pb
P1	0.2	14.6	9.1	76.1	0
P2	10.2	11.6	7.1	64.9	6.3
P3	14.4	11.8	7.1	59.3	7.4
P4	4.2	13.2	8.4	69.2	5
P5	2.3	14.1	8.7	67.4	7.4
P6	3	10.1	6.7	69.2	11.1
P7	3.6	14.9	9.3	61.4	10.8
P8	0.2	14.6	9.3	75.9	0
P9	0.4	14.8	9.3	75.6	0

Fig. 4. TEM micrograph and chemical compositions of the crack developed for Alloy 600 during the SSRT test in 0.1 M NaOH + PbO at 315 °C.

plex oxide layer formed at the surface in 0.1 M NaOH solution without lead was more passive than the single layer formed in the leaded 0.1 M NaOH solution. According to the previous report [10], the Ni-rich outer layer is porous and the Cr-rich inner layer is dense. Thus, it is conceived that the absence of passive and dense Cr-rich oxide for Alloy 600 is responsible for the SCC susceptibility in the leaded 0.1 M NaOH solution.

Fig. 3 presents the TEM-EDS results for the Alloy 690 immersed in the unleaded 0.1 M NaOH solution (Fig. 3a) and in the leaded solution (Fig. 3b). The outer and inner oxides are Ni-rich oxide and relatively Cr-rich oxide (up to 70 wt.%), respectively, in the unleaded 0.1 M NaOH solution while a single layer was observed in the leaded 0.1 M NaOH solution in spite of chemical compositional variation with the distance, which is similar with the results of Alloy 600. In the leaded solution, a large amount of lead was observed up to 35% on the surface leading to the Ni depletion in the oxide layer. The Cr concentration in the oxide formed in the leaded 0.1 M NaOH solution was higher (≥ 30 wt.%) than the concentration of Alloy 690 matrix. It should be noted that the Cr content for Alloy 690 is higher than that for Alloy 600 in leaded 0.1M NaOH solution. The Cr is effectively used as an alloying element of Ni- and Fe-based alloys because of the superior corrosion resistance of Cr oxide [11,12].

Therefore the higher Cr can form more stable oxide in Alloy 690 than Alloy 600. It is presumed that the Cr content preserved at a high level in the oxide is closely related with the superior PbSCC resistance of Alloy 690 in the leaded 0.1 M NaOH solution.

Fig. 4 shows TEM micrograph and chemical composition (wt.%) of the crack developed for Alloy 600 during the SSRT test in 0.1 M NaOH + PbO at 315 °C. Wavy crack initiated and propagated in the direction perpendicular to applied tensile stress during the experiment. Pb was observed in the oxide at the tight crack tip as well as crack mouth and

crack wall. It is expected that Pb accelerates an SCC propagation through the effective transport of Pb along the tight crack as well as an SCC initiation through passivity degradation on the free surface.

4. SUMMARY

The passive duplex oxide layer was observed in the 0.1 M NaOH solution while the less passive single oxide layer was obtained in the leaded 0.1 M NaOH solution for Alloy 600.

It was found that the Cr-rich oxide played an important role in SCC resistance from the fact that the SCC resistance of Alloy 690 with the passive Cr-rich oxide in the surface is much higher than that of Alloy 600 without Cr-rich oxide in the surface in leaded 0.1M NaOH solution.

Pb was effectively examined in the oxide at the tight crack tip as well as free surface oxide expecting that Pb accelerates an SCC propagation through the effective transport of Pb along the tight crack as well as an SCC initiation through passivity degradation on the free surface.

ACKNOWLEDGEMENTS

This work was funded by Korea Ministry of Education, Science and Technology (MEST).

REFERENCES

[1] J.M. Sarver, In: *EPRI Workshop on Intergranular Corrosion and Primary Water Stress Corrosion Cracking Mechanisms* (NP-5971, EPRI, Palo Alto, 1987), p. C11/1.

[2] M.L. Castano-Marin, D. Gomez-Briceno and F. Hernandez-Arroyo, In: *Proc. of 6th Int. Symp. on Environmental Degradation of Materials in Nuclear Power Systems-Water Reactors* (San Diego, CA, USA, Aug. 1-5, 1993), p. 189.

[3] M.D. Wright and M. Mirzai, In: *Proc. of 9th Int. Symp. on Environmental Degradation of Materials in Nuclear Power Systems-Water Reactors* (Newport Beach, CA, USA, Aug. 1-5, 1999), p. 657.

[4] R.W. Staehle, In: *Proc. of 11th Int. Symp. on Environmental Degradation of Materials in Nuclear Power Systems-Water Reactors* (Stevenson, WA, USA, Aug. 10-14, 2003), p. 381.

[5] F. Vaillant, D. Buisine, B. Prieux, D. Gomez Briceno and L. Castano, In: *Eurocorr 96* (Nice, France, 1996), p. 13/1.

[6] U.C. Kim, K.M. Kim and E.H. Lee // *J. Nuclear Materials* **341** (2005) 169.

[7] MULTEQ calculation performed at ANL (2008).

[8] M. Pourbaix, *Atlas of Electrochemical Equilibria in Aqueous Solutions* (Pergamon press Ltd, 1966).

[9] D.-J. Kim, H.P. Kim, S.S. Hwang, J.S. Kim and J. Park // *Met. Mater. Int.* **16** (2010) 259.

[10] D.-J. Kim, Y.S. Lim, H.C. Kwon, S.S. Hwang and H.P. Kim // *J. Nanoscience and Nanotech.* **10** (2010) 85.

[11] G. Lu and G. Xangari // *Electrochim. Acta*, **47** (2002) 2969.

[12] H. Ota, S. Kubo, M. Hodotsuka, T. Inatomi, M. Kobayashi, A. Terada, S. Kasahara, R. Hino, K. Ogura and S. Maruyama, In: *13th International Conference on Nuclear Engineering* (Beijing, China, 2005), p. 1.